NASA TECHNICAL NOTE

NASA TN D-3080

ANALYSIS OF CHUGGING IN LIQUID-BIPROPELLANT ROCKET ENGINES USING PROPELLANTS WITH DIFFERENT VAPORIZATION RATES

by Leon M. Wenzel and John R. Szuch

Lewis Research Center

Cleveland, Ohio

NATIONAL AERONAUTICS AND SPACE ADMINISTRATION • WASHINGTON, D. C. • OCTOBER 1965

NASA TN D-3080

ANALYSIS OF CHUGGING IN LIQUID-BIPROPELLANT ROCKET ENGINES USING PROPELLANTS WITH DIFFERENT VAPORIZATION RATES

By Leon M. Wenzel and John R. Szuch

Lewis Research Center
Cleveland, Ohio

NATIONAL AERONAUTICS AND SPACE ADMINISTRATION

For sale by the Clearinghouse for Federal Scientific and Technical Information
Springfield, Virginia 22151 – Price $1.00

ANALYSIS OF CHUGGING IN LIQUID-BIPROPELLANT ROCKET ENGINES USING PROPELLANTS WITH DIFFERENT VAPORIZATION RATES

by Leon M. Wenzel and John R. Szuch

Lewis Research Center

SUMMARY

The model for prediction of low-frequency stability limits for bipropellant rocket engines is modified to include a discrete vaporization time for each propellant, plus a mixing and reaction time common to both propellants. With this modified model as a hypothesis, stability boundaries are calculated for an engine burning liquid oxygen and gaseous hydrogen. The results obtained are, for certain combinations of vaporization and mixing times, converse to those which would be obtained by a lumped-dead-time model such as has been used. For these cases in particular, stability can be improved by decreasing the hydrogen-injector pressure drop, or by increasing the oxygen-vaporization time. Until now, these two concepts have been diametrically opposed to design criteria for stability improvement. The limited data that exist qualitatively support the modified model.

For simplicity, factors such as a complex feed system and sensitivity of the dead times to chamber pressure and injection velocity are not included in this analysis.

INTRODUCTION

Low-frequency stability of liquid-propellant rocket engines has been the subject of many analyses during the past two decades. The analytical models currently in use to predict stability limits have evolved from the contributions of many researchers. Von Karman (ref. 1) introduced the concept of a combustion delay (dead time) as an explanation of chamber pressure oscillations, Gunder and Friant (ref. 2) added feed system inertance, and Summerfield (ref. 1) introduced combustion chamber dynamics to the model. Crocco and Cheng (ref. 3) refined the model by letting the dead time vary with chamber pressure, and Hurrell (ref. 4) added injection velocity effects.

In previous analyses, the vaporization time of the propellant having the longer drop

lifetime was calculated in the manner of Priem and Heidmann (ref. 5). This vaporization time, generally referred to as dead time, was then applied to both propellants. In rocket engines where the propellants have radically different drop lifetimes or where one of the propellants is introduced as a gas, stability models with a common dead time yield questionable results.

This report advances a stability model in which each propellant is acted on by a discrete dead time. This concept is used in the development of the equations describing the stability boundaries, and typical analytical results are presented. Since it is the purpose of this report to stress the importance of discrete dead times, neither the effects of the feed system nor the pressure and velocity sensitivity of the dead times will be considered.

ANALYSIS

Combustion Process

The combustion process in a liquid-propellant rocket engine is still not clearly understood, although what takes place is generally known. Initially, the propellants are injected into the combustion chamber; their flow rates are determined by the conditions upstream and downstream of the injector element and the element geometry. The propellants are atomized, vaporized, and mixed, and then they react to produce hot gases. These processes are gradual and continuous. For mathematical expendiency, however, they are treated in a discontinuous manner; that is, the gradual evolution of several small elements of propellants into a particle of burned gas is replaced by a sudden conversion. The time interval between injection and sudden conversion is called dead time. The manner in which dead time is applied to propellants will be critically reviewed in this report.

As noted in reference 1, the time rate of change of chamber pressure is determined by the rate of generation of burned gases and by the rate of depletion of the burned gases through the nozzle. The characteristic time associated with this process is the well-known gas-residence time θ_g.

New Model

In previous analyses, the dead times for all the processes were lumped together and applied equally to both propellants. While it is true that mixing and reaction times are common, vaporization times are associated with individual propellants and should be

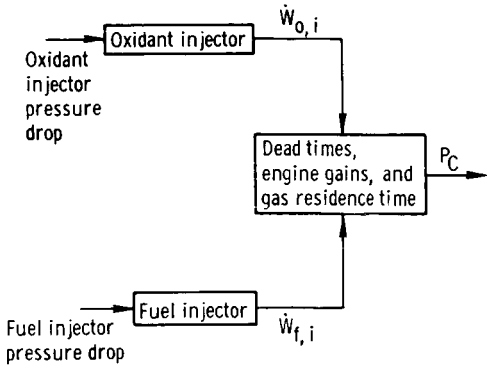

(a) Single-dead-time model.

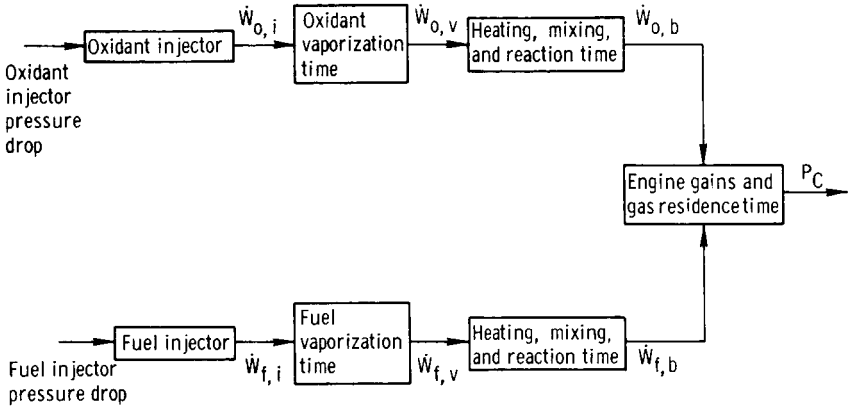

(b) Postulated model.

Figure 1. - Block diagrams for stability limit models for bipropellant rocket engines.

treated accordingly. These concepts are illustrated as block diagrams in figure 1. For comparison, the formerly used single-dead-time model is presented in figure 1(a), and the postulated model with dead times acting on their respective flows is presented in figure 1(b). In this figure, the feed system is assumed to be completely decoupled. It is important to note the discreteness of the dead times, that is, the assigning of different dead times to each flow loop. This is the primary departure from the models used in the past. The following equations describe this model. (Symbols are defined in the appendix.)

By definition

$$P_{T,o}(t) - P_C(t) = \Delta P_{I,o}(t) \tag{1}$$

$$P_{T,f}(t) - P_C(t) = \Delta P_{I,f}(t) \tag{2}$$

The flow through the injectors can be expressed by

$$\dot{W}_{o,i}(t) = K_o \left[\Delta P_{I,o}(t)\right]^a \tag{3}$$

$$\dot{W}_{f,i}(t) = K_f \left[\Delta P_{I,f}(t)\right]^b \tag{4}$$

where the K's and the exponents are assumed to be constant,

$$\dot{W}_{o,v}(t) = \dot{W}_{o,i}(t - \sigma_{v,o}) \tag{5}$$

$$\dot{W}_{f,v}(t) = \dot{W}_{f,i}(t - \sigma_{v,f}) \tag{6}$$

$$\dot{W}_{o,b}(t) = \dot{W}_{o,v}(t - \sigma_m) \tag{7}$$

$$\dot{W}_{f,b}(t) = \dot{W}_{f,v}(t - \sigma_m) \tag{8}$$

By conservation of mass,

$$\frac{d}{dt}\left[W_s(t)\right] = \dot{W}_{o,b}(t) + \dot{W}_{f,b}(t) - \dot{W}_N(t) \tag{9}$$

If the burned products behave as a perfect gas,

$$P_C(t) = \frac{RT_C}{V_C} W_s(t) \tag{10}$$

For a choked nozzle

$$\dot{W}_N(t) = \frac{P_C(t)Ag}{C^*(t)} \tag{11}$$

After linearization and/or Laplace transformation, these equations become

$$\delta\dot{W}_{o,i}(s) = \overline{\frac{dW_{o,i}}{d\Delta P_{I,o}}} \left[\delta P_{T,o}(s) - \delta P_C(s)\right] \tag{12}$$

$$\delta\dot{W}_{f,i}(s) = \overline{\frac{dW_{f,i}}{d\Delta P_{I,o}}} \left[\delta P_{T,f}(s) - \delta P_C(s)\right] \tag{13}$$

$$\delta\dot{W}_{o,v}(s) = \delta\dot{W}_{o,i}(s)e^{-\sigma_{v,o}s} \tag{14}$$

$$\delta\dot{W}_{f,v}(s) = \delta\dot{W}_{f,i}(s)e^{-\sigma_{v,f}s} \tag{15}$$

$$\delta\dot{W}_{o,b}(s) = \delta\dot{W}_{o,v}(s)e^{-\sigma_{m}s} \tag{16}$$

$$\delta\dot{W}_{f,b}(s) = \delta\dot{W}f,_{v}(s)e^{-\sigma_{m}s} \tag{17}$$

$$\partial P_C(s) = \frac{1}{\theta_g s + 1}\left[\left(\frac{\overline{\partial P_C}}{\partial \dot{W}_o}\right)\delta\dot{W}_{o,b}(s) + \left(\frac{\overline{\partial P_C}}{\partial \dot{W}_f}\right)\delta\dot{W}_{f,b}(s)\right] \tag{18}$$

The gas residence time θ_g is defined as

$$\theta_g = \frac{C^*V_C}{RT_CAg} = \frac{C^*L^*}{RT_Cg} \tag{19}$$

and is assumed to be constant.

Equation (10) to (17) can be combined to yield

$$\delta P_C(s) = \left\{\left(\frac{\overline{\partial P_C}}{\partial \dot{W}_o}\right)\left(\frac{\overline{d\dot{W}_o}}{d\,\Delta P_{I,o}}\right)\left[\delta P_{T,o}(s) - \delta P_C(s)\right]e^{-(\sigma_m+\sigma_{v,o})s} + \left(\frac{\overline{\partial P_C}}{\partial \dot{W}_f}\right)\left(\frac{\overline{d\dot{W}_f}}{d\,\Delta P_{I,f}}\right)\left[\delta P_{T,f}(s) - \delta P_C(s)\right]e^{-(\sigma_m+\sigma_{v,f})s}\right\}\frac{1}{\theta_g s + 1} \tag{20}$$

Solving for $\delta P_C(s)$ yields

$$\delta P_C(s) = \frac{\left[\left(\frac{\overline{\partial P_C}}{\partial \dot{W}_o}\right)\left(\frac{\overline{d\dot{W}_o}}{d\,\Delta P_{I,o}}\right)e^{-(\sigma_m+\sigma_{v,o})s}\delta P_{T,o}(s) + \left(\frac{\overline{\partial P_C}}{\partial \dot{W}_f}\right)\left(\frac{\overline{d\dot{W}_f}}{d\,\Delta P_{I,f}}\right)e^{-(\sigma_m+\sigma_{v,f})s}\delta P_{T,f}(s)\right]\frac{1}{\theta_g s+1}}{1 + \frac{1}{\theta_g s + 1}\left[\left(\frac{\overline{\partial P_C}}{\partial \dot{W}_o}\right)\left(\frac{\overline{d\dot{W}_o}}{d\,\Delta P_{I,o}}\right)e^{-(\sigma_m+\sigma_{v,o})s} + \left(\frac{\overline{\partial P_C}}{\partial \dot{W}_f}\right)\left(\frac{\overline{d\dot{W}_f}}{d\,\Delta P_{I,f}}\right)e^{-(\sigma_m+\sigma_v)s}\right]} \tag{21}$$

The denominator of equation (19) is, when set equal to zero, the characteristic equation

$$0 = 1 + \frac{e^{-\sigma_m s}}{\theta_g s + 1}\left[\left(\overline{\frac{\partial P_C}{\partial \dot{W}_o}}\right)\left(\overline{\frac{d\dot{W}_o}{d\,\Delta P_{I,o}}}\right)e^{-\sigma_{v,o} s} + \left(\overline{\frac{\partial P_C}{\partial \dot{W}_f}}\right)\left(\overline{\frac{d\dot{W}_f}{d\,\Delta P_{I,f}}}\right)e^{-\sigma_{v,f} s}\right] \tag{22}$$

(see, e.g., ref. 6). Evaluating the derivatives results in

$$\overline{\frac{d\dot{W}_o}{d\,\Delta P_{I,o}}} = a\overline{K}_o\,\overline{\Delta P}_{I,o}^{a-1} = a\,\frac{\overline{\dot{W}}_o}{\overline{\Delta P}_{I,o}} \tag{23}$$

Since $\overline{K}_o = (\overline{W}_o/\overline{\Delta P}_{I,o}^{a})$, and

$$\overline{\frac{d\dot{W}_f}{d\,\Delta P_{I,f}}} = b\,\frac{\overline{\dot{W}}_f}{\overline{\Delta P}_{I,f}} \tag{24}$$

$$P_C = \frac{C^*}{Ag}\left(\dot{W}_{o,b} + \dot{W}_{f,b}\right) \tag{25}$$

$$\frac{\partial P_C}{\partial \dot{W}_{o,b}} = \frac{1}{Ag}\left[\overline{C^*} + \left(\overline{\dot{W}_{o,b}} + \overline{\dot{W}_{f,b}}\right)\frac{\partial C^*}{\partial W_{o,b}}\right] \tag{26}$$

$$\frac{\partial C^*}{\partial \dot{W}_{o,b}} = \frac{\partial C^*}{\partial R}\,\frac{dR}{d\dot{W}_{o,b}} = \frac{\partial C^*}{\partial R}\,\frac{1}{W_{f,b}} \tag{27}$$

where $R = \dot{W}_{o,b}/\dot{W}_{f,b}$, and

$$\overline{\frac{\partial P_C}{\partial \dot{W}_{o,b}}} = \frac{1}{Ag}\left[\overline{C^*} + (\overline{R} + 1)\,\overline{\frac{\partial C^*}{\partial R}}\right] \tag{28}$$

In like manner,

$$\overline{\frac{\partial P_C}{\partial \dot{W}_{f,b}}} = \frac{1}{Ag}\left[\overline{C^*} - \overline{R}(\overline{R} + 1)\,\overline{\frac{\partial C^*}{\partial R}}\right] \tag{29}$$

Substituting equations (23), (24), (28), and (29) into equation (22) gives

$$-1 = \frac{1}{Ag}\frac{e^{-\sigma_m s}}{\theta_g s + 1}\left\{\frac{a\overline{W}_o}{\Delta P_{I,o}}\left[\overline{C^*} + (\overline{R}+1)\frac{\overline{\partial C^*}}{\partial R}\right]e^{-\sigma_{v,o}s} + \frac{b\overline{W}_f}{\Delta P_{I,f}}\left[\overline{C^*} - \overline{R}(\overline{R}+1)\frac{\overline{\partial C^*}}{\partial R}\right]e^{-\sigma_{v,f}s}\right\} \tag{30}$$

Equation (30) rewritten in terms of $\overline{\Delta P_I}/\overline{P_C}$ is

$$-1 = \frac{e^{-\sigma_m s}}{\theta_g s + 1}\left[e^{-\sigma_{v,o}s}\,\frac{a}{\frac{\overline{\Delta P_{I,o}}}{\overline{P_C}}}\left(\frac{\overline{R}}{\overline{R}+1} - \overline{R}\,\frac{\overline{\frac{\partial C^*}{\partial R}}}{\overline{C^*}}\right) + e^{-\sigma_{v,f}s}\,\frac{b}{\frac{\overline{\Delta P_{I,f}}}{\overline{P_C}}}\left(\frac{1}{\overline{R}+1} - \overline{R}\,\frac{\overline{\frac{\partial C^*}{\partial R}}}{\overline{C^*}}\right)\right] \tag{31}$$

Equation (31) may be reduced to a single-dead-time case by setting $\Delta_{v,o}$ equal to $\Delta_{v,f}$ and combining with Δ_m so that

$$-1 = \frac{e^{-\sigma s}}{\theta_g s + 1}\left[\frac{a}{\frac{\overline{\Delta P_{I,o}}}{\overline{P_C}}}\left(\frac{\overline{R}}{\overline{R}+1} - \overline{R}\,\frac{\overline{\frac{\partial C^*}{\partial R}}}{\overline{C^*}}\right) + \frac{b}{\frac{\overline{\Delta P_{I,f}}}{\overline{P_C}}}\left(\frac{1}{\overline{R}+1} - \overline{R}\,\frac{\overline{\frac{\partial C^*}{\partial R}}}{\overline{C^*}}\right)\right] \tag{32}$$

RESULTS

Equation (31) may be implemented on a digital computer to solve for engine stability. For example, consider an engine running on gaseous hydrogen and liquid oxygen. Since the hydrogen enters the chamber as a gas, fuel vaporization time is zero. In figure 2, stability boundaries are presented for an oxidant vaporization time of 2 milliseconds and mixing times varying between 0 and 4 milliseconds. A point on the stability boundary is determined by those values of $\overline{\Delta P_{I,f}}/\overline{P_C}$ and $\overline{\Delta P_{I,o}}/\overline{P_C}$ which yield one or more conjugate pairs of roots of equation (29) which lie on the imaginary axis ($s = \alpha + j\omega$; $\alpha = 0$), with the condition that no roots exist to the right of the imaginary axis ($s = \alpha + j\omega$; $\alpha > 0$). The stability boundaries are presented as loci of these points.

In figure 2, the stable operating region lies above and/or to the right of the boundary in each case. It is seen that, as mixing time is decreased, the area of stable operation increases. Furthermore, the shape of the curves becomes such that a transition from unstable to stable operation can be achieved by decreasing the fuel pressure drop. Although contrary to the usual practice of increasing pressure drops to stabilize an engine, this concept is in agreement with experimental experience on an engine of this type (ref. 7) where this exact behavior was observed.

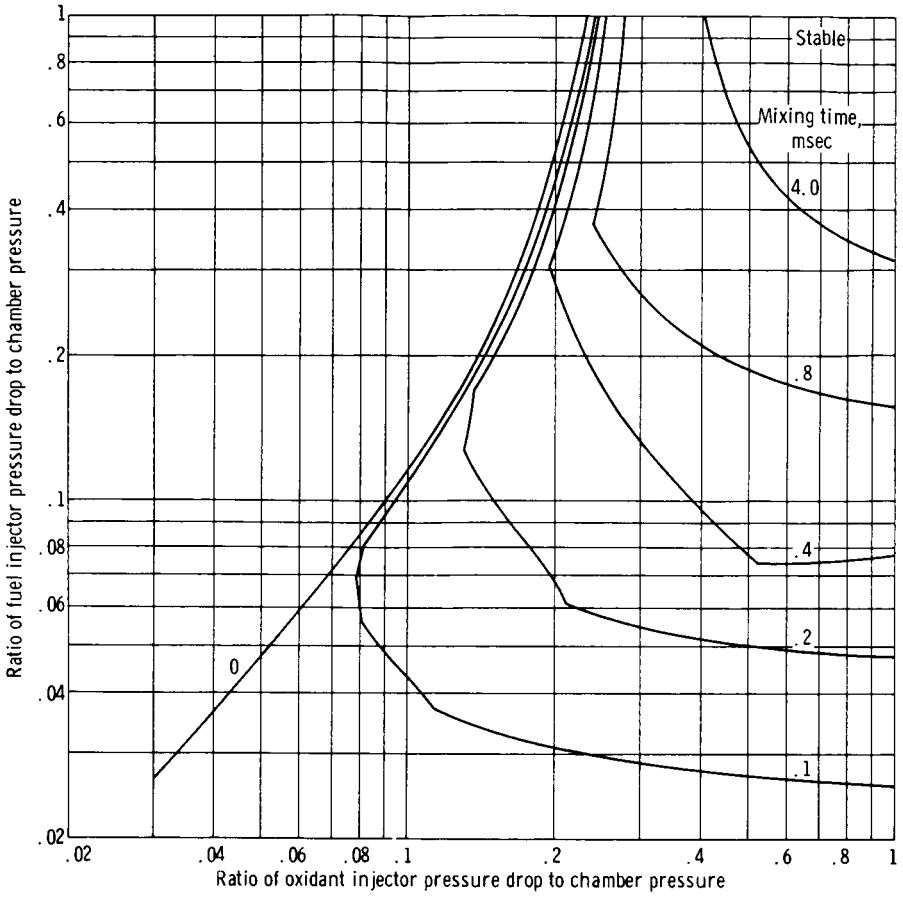

Figure 2. - Effect of mixing time on stability boundary. Vaporization time, 2.0 milliseconds.

The frequency at which the oscillations occur changes along the curve, although this fact is not indicated in figure 2. The discontinuities in the curves (for mixing times between 0.1 and 0.8 msec) correspond to a flip in frequency from one mode to another. At the inflection points, two pairs of roots exist on the imaginary axis and oscillations occur at both the associated frequencies.

Study of the behavior predicted by this model indicates that stability may be achieved by manipulation of the dead times. This point is illustrated in figure 3. Mixing dead time is held constant at 1.0 millisecond, and stability boundaries are plotted for vaporization dead times ranging from 0.5 to 2.0 milliseconds. Again, the stable region lies above and/or to the right of each curve. If the operating point indicated by the symbol were chosen, a transition from unstable to stable operation could be realized by increasing the oxidant vaporization time from some lower value to 1.5 milliseconds. This behavior is contrary to that which would be predicted by a single-dead-time model, where any increase in dead time adversely affects stability. It should be pointed out, however, that further increases in dead time are destabilizing.

The behavior predicted by the single-dead-time model, which is described by equa-

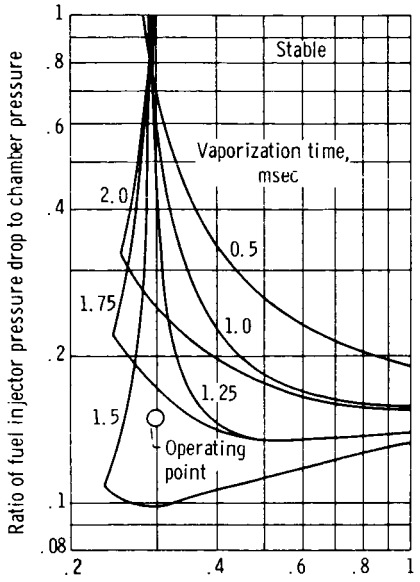

Figure 3. - Effect of vaporization time on stability boundary. Mixing time, 1.0 millisecond.

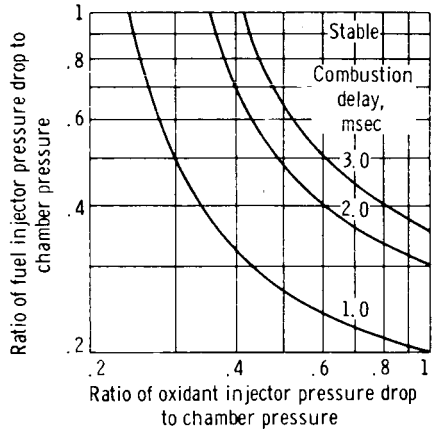

Figure 4. - Stability boundaries calculated with single-dead-time model.

tion (32), is illustrated in figure 4 for mixing times ranging from 1.0 to 3.0 milliseconds. For this model, any increase in dead time, or decrease in pressure drop, is destabilizing.

CONCLUDING REMARKS

This report has advanced the concept of separate dead times and demonstrated the effects of using this concept in chugging analyses. Since the presentation of results would have been encumbered by variables such as a complex feed system and the sensitivity of the dead times to pressure and injection velocity, these effects have not been included.

There are limited experimental data to qualitatively substantiate the behavior predicated by this model. The model does, however, provide an explanation for the data in reference 7, where chugging was eliminated by decreasing the fuel injector pressure drop. This result is inexplicable when a single-dead-time model is used.

Reference 8 indicates that, for hydrogen-oxygen engines, a low oxygen-injection velocity is desirable from a screeching standpoint. This implies a long oxygen-vaporization time, which has previously been deemed undesirable from a chugging point of view. The model advanced herein indicates that a long vaporization time may not be

undesirable; hence, an injector with a low propensity to screech may not compromise low-frequency stability.

If the performance predicted by this model is corroborated as additional data are obtained, currently used design criteria such as maintaining a minimum $\overline{\Delta P}/\overline{P}_C$ and striving for low vaporization times should be critically reviewed.

Lewis Research Center,
National Aeronautics and Space Administration,
Cleveland, Ohio, August 5, 1965.

APPENDIX

SYMBOLS

A	throat area, $in.^2$
a	exponent of oxidant injector
b	exponent of fuel injector
C*	characteristic exhaust velocity, in./sec
g	gravity, $in./sec^2$
j	$\sqrt{-1}$
K	injector resistance constant
L*	characteristic chamber length, in.
P	pressure, $lb/in.^2$ abs
R	mixture ratio, $\dot{W}_o/\dot{W}_f$
$\mathcal{R}$	gas constant, $in./^oR$
s	Laplace operator, 1/sec
T	temperature, ^oR
t	time, sec
V	volume, $in.^3$
W	weight, lb
$\dot{W}$	propellant flow rate, lb/sec
α	real part of Laplace operator, s
δ	perturbation
θ_g	gas residence time, sec
σ	dead time, sec
ω	imaginary part of Laplace operator, s

Subscripts:

b	burned
C	chamber
f	fuel
I	injector
i	injected
m	mixing, reaction, and heating
N	nozzle
o	oxidant
s	stored
T	tank
v	vaporized, vaporization

REFERENCES

1. Summerfield, Martin: A Theory of Unstable Combustion in Liquid Propellant Rocket Systems. J. Am. Rocket Soc., vol. 21, no. 5, Sept. 1951, pp. 108-114.

2. Gunder, D. F.; and Friant, D. R.: Stability of Flow in a Rocket Motor. J. Appl. Mech., vol. 17, no. 3, Sept. 1950, pp. 327-333.

3. Crocco, Luigi; and Cheng, Sin-I: Theory of Combustion Instability in Liquid Propellant Rocket Motors. AGARDograph No. 8, Butterworths Sci. Pub. (London), 1956.

4. Hurrell, Herbert G.: Analysis of Injection-Velocity Effects on Rocket Motor Dynamics and Stability. NASA TR R-43, 1959.

5. Priem, Richard J.; and Heidmann, Marcus F.: Propellant Vaporization as a Design Criterion for Rocket-Engine Combustion Chambers. NASA TR R-67, 1960.

6. Kuo, Benjamin C.: Automatic Control System. Prentice-Hall, Inc., 1962.

7. Anon.: J-2 Program Quarterly Progress Report for Period Ending February 28, 1962. Rept. No. R-2600-6, Rocketdyne, North Am. Aviation, 1962, pp. 85; 137-140.

8. Bloomer, Harry E.: 20K H-O Screech Work at Lewis. CPIA Pub. No. 66, Vol. 1, Abstracts of the 1st Combustion Instability Conf., Chem. Prop. Info. Agency, Nov. 1964, p. 16.